Development/Plasticity/Repair

Caspase-7 Expanded Function and Intrinsic Expression Level Underlies Strain-Specific Brain Phenotype of *Caspase-3*-Null Mice

Caroline Houde,[1] Kathleen G. Banks,[2] Nathalie Coulombe,[3] Dita Rasper,[3] Erich Grimm,[3] Sophie Roy,[1,4] Elizabeth M. Simpson,[2] and Donald W. Nicholson[1,4]

[1]Biochemistry Department, McGill University, Montreal, Quebec H3G 1Y6, Canada, [2]Centre for Molecular Medicine and Therapeutics, British Columbia Institute for Children's and Women's Health, Department of Medical Genetics, University of British Columbia, Vancouver, British Columbia V5Z 4H4, Canada, [3]Merck Frosst Canada and Company, Pointe-Claire–Dorval, Quebec H9R 4P8, Canada, and [4]Merck Research Laboratories, San Diego, California 92121

Caspase-3-deficient mice of the 129S1/SvImJ (129) strain show severe brain development defects resulting in brain overgrowth and perinatal lethality, whereas on the C57BL/6J (B6) background, these mice develop normally. We therefore sought to identify the strain-dependent ameliorating gene. We biochemically isolated caspase-7 from B6-caspase-3-null (*Casp3*$^{-/-}$) tissues as being the enzyme with caspase-3-like properties and capability of performing a caspase-3 surrogate function, apoptotic DNA fragmentation. Moreover, we show that, in contrast to the human enzymes, mouse caspase-7 is as efficient as caspase-3 at cleaving and thus inactivating ICAD (inhibitor of caspase-activated DNase), the inhibitor of apoptotic DNA fragmentation. Low levels of caspase-7 expression and activation correlate with lack of DNA fragmentation in 129-*Casp3*$^{-/-}$ apoptotic precursor neurons, whereas B6-*Casp3*$^{-/-}$ cells, which can fragment their DNA, show higher levels of caspase-7 expression and activation. The amount of caspase-7 activation in apoptotic precursor neurons is independent of the presence of caspase-3. Together, our findings demonstrate for the first time a strong correlation between caspase-7 activity, normal brain development, and apoptotic DNA fragmentation in *Casp3*$^{-/-}$ mice.

Key words: **apoptosis; brain development; strain-specific phenotype; caspase-3 compensation; caspase-7; DNA fragmentation**

Introduction

Apoptosis, or programmed cell death, is mediated by the activation of caspases (Casp), a family of cysteine proteases present as proenzymes in all cells and activated by cleavage and reorganization of their subunits after an intracellular or extracellular apoptotic signal (Nicholson, 1999). Caspases orchestrate the organized death of the cell by cleaving a small but specific complement of protein substrates. One of the best characterized morphological changes resulting from caspase substrate cleavage is DNA fragmentation at internucleosomal intervals (Wyllie, 1980; Nagata et al., 2003). Caspase-activated DNase (CAD), the DNase responsible for apoptotic DNA fragmentation, is translated in the cytoplasm where it is stabilized by its cognate chaperone and inhibitor ICAD (Sakahira et al., 2000). Once activated, the well characterized executioner caspase, caspase-3, cleaves ICAD, releasing inhibition of CAD, which then translocates to the nucleus where it fragments DNA (Sakahira et al., 1998).

Received May 12, 2004; revised Sept. 16, 2004; accepted Sept. 17, 2004.

C.H. was supported by the Canadian Institutes of Health Research. E.M.S. is supported by a Merck Frosst grant to the Centre for Molecular Medicine and Therapeutics and is a holder of a Canada Research Chair in Genetics and Behavior. We thank Dr. S. Nagata for the mICAD construct.

Correspondence should be addressed to D. W. Nicholson, Merck Research Laboratories–San Diego, 3535 General Atomics Court, MRL SDB1, San Diego, CA 92121. E-mail: donald_nicholson@merck.com.

DOI:10.1523/JNEUROSCI.3356-04.2004

 0270-6474/04/249977-08$15.00/0

A balance between the proliferation of neural progenitors and apoptotic cell death is essential for proper brain development (Kuan et al., 2000). In the mouse, targeted deletion of *caspase-3* (Kuida et al., 1996), *caspase-9* (Hakem et al., 1998; Kuida et al., 1998), or *apaf-1* (a coactivator of caspase-9) (Cecconi et al., 1998; Yoshida et al., 1998) genes, yet not of other caspases, results in brain development defects. In all cases, supernumerary cells in the forebrain and midbrain cause neural tissue protrusions through the skull as a result of defects in apoptotic cell death. *Apaf*$^{-/-}$ embryos do not survive past embryonic day 16.5 (E16.5) when they are from a mixed 129/Sv-CP-NMRI genetic background (Cecconi et al., 1998), but some embryos do survive for a few days when on a mixed 129/O1a-C57BL/6 or 129/Ola-CD1 background (Yoshida et al., 1998). *Casp3*$^{-/-}$ and *Casp9*$^{-/-}$ mice of a mixed 129/Sv-C57BL/6 or 129/O1a-C57BL/6J background are born, albeit at a lower frequency than the expected Mendelian ratio. Most live-born pups die within a few weeks, but a few survive and age with no apparent gross abnormalities. Variabilities in phenotype might be reflective of strain-specific modifier genes that affect the apoptotic program.

We report here that the *Casp3*-deletion phenotype is strain specific. The C57BL16J (B6) strain is resistant to loss of caspase-3, whereas the 129S1/SvImJ (129) strain develops severe brain defects. Using a biochemical approach to investigate the molecular mechanism responsible for the resistance of the B6 strain to the

loss of caspase-3, we identified caspase-7 as having similar properties to caspase-3 in the mouse. Although caspase-7 is expressed in both strains during brain development, its expression level is lower in 129 compared with B6 brains. Lower levels of caspase-7 expression and activation in precursor neurons from 129-*Casp3*$^{-/-}$ mice correlate with lack of DNA fragmentation, whereas B6-*Casp3*$^{-/-}$ cells with higher intrinsic caspase-7 levels can fragment their DNA. This is the first report supporting a role for caspase-7 in brain development and DNA fragmentation in the absence of caspase-3.

Materials and Methods

Congenic derivation and genotyping. Mice deleted for *Casp3* were generated as described previously (*Casp3*^{tm1Mr1}) (Keramaris et al., 2000). Briefly, a targeting vector containing both the *lacZ-PGKneo* (β-galactosidase–phosphglycerate kinase–neomycin phosphotransferase) and the bacterial diphtheria toxin α-subunit gene driven by the *PGK* promoter was constructed to remove most of exon 5, intron 5, and exon 6. Germline chimeras were generated by injecting the targeted RW4 embryonic stem cells into C57BL/6J blastocysts, and PCR was used to confirm homozygous disruption of the *Casp3* gene. Two male *Casp3*$^{+/-}$ at backcross generation (N7) on C57BL/6NTac were backcrossed onto both B6 and 129. Experimental animals were backcrossed 4–10 generations onto the B6 strain and 4–14 generations onto the 129 strain. Genotyping for the *Casp3* wild-type (WT) and knock-out (KO) alleles was performed on DNA from adult tail or ear biopsy or embryo tail, paw, or yolk sac by PCR using the previously described oligonucleotide pairs (Vanderluit et al., 2000). Specifically, the WT *Casp3* allele 5′ primer 5′-AAGCTGTCTTCGTCCAGTGAG-3′ (oEMS1051) corresponding to base pairs 3122–3142, and the 3′ primer 5′-CTAAGTTAACCAAACTGAGCACCGC-3′ (oEMS905) corresponding to base pairs 3475–3451, generated a band of 353 bp. Primers for the KO allele used the same 5′ primer (oEMS1051) as the WT gene, and the 3′ primer 5′-GTCGATCCACTAGTTCTAGAGCGGC-3′ (oEMS904) corresponded to the multiple cloning site of the inserted DNA, which generated a band of 223 bp. All PCR reactions used the following conditions: 94°C for 2 min, 30 cycles of 94°C for 30 sec, 60°C for 1 min, 72°C for 1 min, 72°C extension for 5 min. PCR products were electrophoresed and visualized under standard conditions.

Embryo collection. Timed mating of heterozygous animals from the backcross colonies was used to generate embryos at various gestational ages, such that *Casp3*$^{-/-}$ and *Casp3*$^{+/+}$ embryos were littermates. Fertilization was assumed to have occurred at midnight so that the following mid-day was designated E0.5 of gestation. At the desired gestational ages, the embryos were dissected from the uterus and placed individually in 35 mm dishes containing sterile 1× PBS. Dissected embryos were photographed using a Leica (Nussloch, Germany) MZAPO dissecting microscope and DCF400 camera system. All other tissues were snap frozen in liquid nitrogen immediately after dissection.

Splenocyte culture. Spleens were homogenized in 50 μm Medicon and Medimachine (Dako, Glostrup, Denmark) in Invitrogen (San Diego, CA) culture media RPMI-1640 supplemented with 5% FBS, 2 mM L-glutamine, 200 U/ml penicillin, and 200 μg/ml streptomycin (Invitrogen) for a 25 sec pulse. Cell suspensions were filtered through a 50 μm filcon (Dako). Red blood cells were removed by centrifugation through a Ficoll-Paque layer. Twenty thousand splenocytes were plated per well of a 96-well plate. Apoptosis was induced with 1 mM cycloheximide added to the culture media for 4 hr with or without adding the caspase-3 inhibitor M-791 (see Fig. 2*A*) (Hotchkiss et al., 2000) (Merck Frosst Canada, Montreal, Quebec, Canada). The Cell Death ELISA kit (Roche, Indianapolis, IN) was used to measure DNA fragmentation in lysates from equivalent cell number.

Tissue extracts. Fresh-frozen tissues were homogenized in lysis buffer (50 mM Tris, pH 7.5, 1% NP-40, 2 mM EDTA, 5 mM DTT added fresh, and the Complete protease inhibitor mixture containing 1.5 μg/ml chymotrypsin, 0.8 μg/ml thermolysin, 1 mg/ml papain, 1.5 μg/ml pronase, 1.5 μg/ml pancreatic extract, and 0.002 μg/ml trypsin; Roche) on ice with a 8 mm probe on the Polytron Brinkmann homogenizer (Lucerne, Switzerland). Lysates were cleared by 10 min centrifugation at 10,000 × *g* at 4°C. Cleavage activity at the caspase-3 aspartate-glutamate-valine-aspartate recognition site (DEVDase) was measured for 96 and 48 μg of proteins for each tissue after pretreatment of the extracts with granzyme B for 5 min at 37°C. For E9.5 and E12.5 heads and brains, DTT was omitted, and they were homogenized using a plastic pellet pestle for 1.5 ml tubes (Kontes, Vineland, NJ).

DEVDase activity assay. Protein extracts, purified recombinant enzymes, or chromatography fractions were mixed with a final concentration of 10 μM Ac-DEVD-AMC (acetyl-aspartate-glutamate-valine-aspartate-amino-methyl-coomasin) (Biomol, Plymouth Meeting, PA) in a final volume of 200 μl in buffer consisting of 50 mM HEPES-KOH, 2 mM EDTA, 10% glycerol (v/v), 0.1% 3-[(3-cholamidopropyl) dimethylammonio]-1-propanesulfonate (CHAPS), and 5 mM DTT added fresh. The caspase-3 inhibitor M-791 (Merck Frosst Canada) was added at concentrations ranging from 2.5 μM to 10 pM. Liberation of AMC resulting from cleavage at the caspase-3 consensus site DEVD was scored by the CytoFluor (PerSeptive Biosystems, Framingham, MA) for 60 min at room temperature (excitation, 380 nm; emission, 460 nm).

Chromatography. Livers, kidneys, and spleens were homogenized with an 8 mm probe on the Polytron Brinkmann homogenizer on ice in ICE III buffer (50 mM HEPES-KOH, pH 7.0, 2 mM EDTA, 10% sucrose, 0.1% CHAPS, and 5 mM DTT added fresh). Cells were broken by 25 stokes in a ground glass dounce. Lysates were cleared by two centrifugations at 10,000 × *g* for 30 min and an ultra-centrifugation at 100,000 × *g* for 1 hr. Extracts were activated by granzyme B pretreatment before loading into a Mono-Q HR 5/5 anion exchange column (Pharmacia, Uppsala, Sweden). Elution was performed with a NaCl gradient ranging from 0 to 0.8 M. Fractions of 1 ml were collected, of which 10 μl were tested for DEVDase activity.

Biotin labeling. DEVDase activity-containing ion exchange chromatography fractions were pooled. The sample was separated into two; one-half was labeled with 10 μM Biotin-DEVD-AOMK (Merck Frosst Canada and Co.) for 30 min at 37°C, and the other half was incubated with DMSO only. After protein separation on a 10–20% SDS-PAGE gel (Invitrogen) and transfer to a nitrocellulose membrane, biotin-labeled peptides were detected by blotting with streptavidin-HRP (Amersham, Little Chalfont, UK) 1:10,000 in 1% BSA in Tris-buffered saline with 0.1% Tween 20 (TBST 0.1%) for 1 hr. The same membrane was blotted with a monoclonal antibody against caspase-7 (see *Reagents*) in 5% milk in 0.1% TBST and a secondary antibody anti-mouse-HRP (Amersham).

Constructs. Mouse caspase-7 cDNA sequence was amplified by PCR from the cDNA clone IMAGE 1498931 with the following forward and reverse primers inserting *Afl*III sites compatible with *Nco*I sites: 5′-GCTCTAGAGGATTCACATGTCCGATGATCAGGACTGTGCTGCGG-3′, 5′-CGTCTAGAGGATCCACATGTTCAACGGCTGAAGTACAGCTCTTTGG-3′. Mouse caspase-7 was cloned into the *Nco*I site of the pET11d vector (Novagen, San Diego, CA) to allow expression in BL21codon+ bacteria after isopropyl-β-D-thiogalactopyranoside induction. Bacterial pellets were lysed in ICE III buffer and sonicated. Caspase-7 was activated by treating the bacterial lysates with granzyme B, and activity was measured by DEVDase assay. The mouse ICAD construct in pBS-SK$^+$ was a kind gift from Dr. Shigekazu Nagata (Osaka University Medical School, Osaka, Japan). The human ICAD cDNA sequence was amplified by PCR from the cDNA clones CS0DC021YD20 and IMAGE 4553902 with the following forward and reverse primers inserting *Eco*RI for cloning into the pBS-SK$^+$ vector: 5′-GCGCGAATTCATGGAGGTGACCGGGGACGCCGGGGTACCAGAAT-3′, 5′-GCGCGAATTCCTATGTGGGATCCTGT-3′.

In vitro *ICAD cleavage.* Human and mouse ICAD were transcribed-translated with the coupled TNT system (Promega, Madison, WI) in the presence of [^{35}S]-methionine (Amersham) according to the manufacturer instructions. Two and one-half microliters of the reactions were subjected to cleavage by purified caspases in a final volume of 20 μl in ICE III buffer. Reactions were incubated at 37°C for 1 hr and stopped by adding Laemmli sample buffer. Proteins were separated on a 10–20% SDS-PAGE gel (Invitrogen) that was then fixed for 15 min in 40% methanol, 10% acetic acid, soaked for 15 min in Enlightning (NEN Life Science Products, Boston, MA), dried under vacuum, and exposed to Kodak (Rochester, NY) Biomax film for 18 hr.

Telencephalic vesicles culture. Precursor neurons from the telencepha-

lon of E12.5 embryos were prepared as described previously (Flaris et al., 1995) with modifications. Briefly, telencephalic vesicles were isolated in cold dissociation medium (DM) [HBSS Ca-Mg Free (Invitrogen) supplemented with 15 mM HEPES (Sigma, St. Louis, MO), 2.7 mM Na bicarbonate (Invitrogen), and 6 gm/l glucose]. Cells were dissociated by incubating in DM supplemented with 0.05% trypsin-0.02% EDTA (Invitrogen), 0.02 mg/ml DNase I, and 0.1% BSA fraction V (Sigma) for 25 min at 37°C. Trypsin was inactivated by adding FBS to a 5% final concentration. Tissues were triturated by pipetting five times with a fire-polished Pasteur pipette. Cells were washed once in DM. Twenty five thousand cells per well of a 96-well plate or 300,000 cells per well of a 12-well plate (poly-D-lysine-coated plates; Biocoat, Bedford, MA) were seeded in DMEM (Invitrogen) supplemented with 25 μM L-glutamic acid, 10 mM HEPES (Sigma), 0.5 mM L-glutamine, 100 U/ml penicillin, 100 μg/ml streptomycin, and 1× B27 supplement (Invitrogen). After 16–20 hr in culture, cells were challenged with camptothecin, a DNA topoisomerase I inhibitor well known as an apoptotic stimulator (Sigma), dissolved in DMSO in the same culture media without the L-glutamic acid for 5 hr. DNA fragmentation was monitored with the Cell Death ELISA kit from Roche using the provided control standard.

Reagents. Purified human and mouse caspase-3, human caspase-7, and granzyme B were prepared as described previously (Thornberry et al., 1997) (see *Constructs* for mouse caspase-7). Briefly, the large and small subunits of each caspase were expressed separately in bacteria, purified from inclusion bodies, solubilized in 6 M guanidine HCl, and then rapidly diluted to a final concentration of 100 μg/ml at room temperature under conditions determined to be optimal for each enzyme subunit folding into the active form. Human granzyme B was extracted with NaCl from granules of cultured human natural killer leukemia T-cells. Diluted extracts were loaded onto a Mono-S cation exchange column (Pharmacia) pre-equilibrated in 50 mM MES, pH 6.1, and 25 mM NaCl. Proteins were eluted with a linear gradient up to 1 M NaCl (in 50 mM MES, pH 6.1). Granzyme B eluted at ~0.6 M NaCl and was homogeneous as judged by SDS-PAGE. Antibodies used were monoclonal anti-caspase-7 AAM-127 from Stressgen (Victoria, British Columbia, Canada) (1:2000), monoclonal anti-tubulin B-5-1-2 from Sigma (1:5000), polyclonal anti-caspase-3 R280 (1:3000) (Merck Frosst Canada and Co.), and anti-mouse or anti-rabbit HRP-coupled secondary antibodies from Amersham (1:3000).

Results

129-*Casp3*$^{-/-}$ but not B6-*Casp3*$^{-/-}$ mice show severe brain development defects

Casp3$^{+/-}$ mice from a mixed 129–B6 background were backcrossed for at least four generations onto 129 and B6 backgrounds. The resulting backcrossed *Casp3*$^{+/-}$ were intercrossed to obtain *Casp3*$^{-/-}$ mice of 129 or B6 backgrounds. Gross brain anatomical abnormalities were observed as early as E9.5 for 129 embryos, the stage at which the neural tube has just closed to form the brain (Fig. 1*A*). As the 129-*Casp3*$^{-/-}$ embryos further develop, abnormal growth of the forebrain, midbrain, and hindbrain are observed compared with wild-type littermates. Three types of exencephalies from E18.5 embryos are shown (Fig. 1*A*, 129-*Casp3*$^{-/-}$) as examples of the continuum in phenotypes that were observed. The variable phenotypes most probably result from a stochastic mechanism in which there is a race between brain overgrowth and skull closure (Gunn et al., 1993; Harris and Juriloff, 1999). Apart from the head, 129-*Casp3*$^{-/-}$ E18.5 embryos did not show any gross anatomical abnormalities. E18.5 129-*Casp3*$^{-/-}$ embryos were present at the expected Mendelian ratio (Fig. 1*B*), and they all showed exencephalies. However, only 3% of live-born 129-*Casp3* progeny were homozygotes. All three living 129-*Casp3*$^{-/-}$ pups had brain extracranial protrusions covered by skin and fur. The B6-*Casp3*$^{-/-}$ mice, on the other end, appeared normal at E18.5, were born at the expected Mendelian ratio, and reached adulthood. Only 4 of 36 B6-*Casp3*$^{-/-}$ mice had overt hydrocephalus (data not shown). The B6 strain is therefore more resistant to *Casp3* deletion than the sensitive 129 strain, which develops severe brain abnormalities. These findings are consistent with previous observations (Leonard et al., 2002).

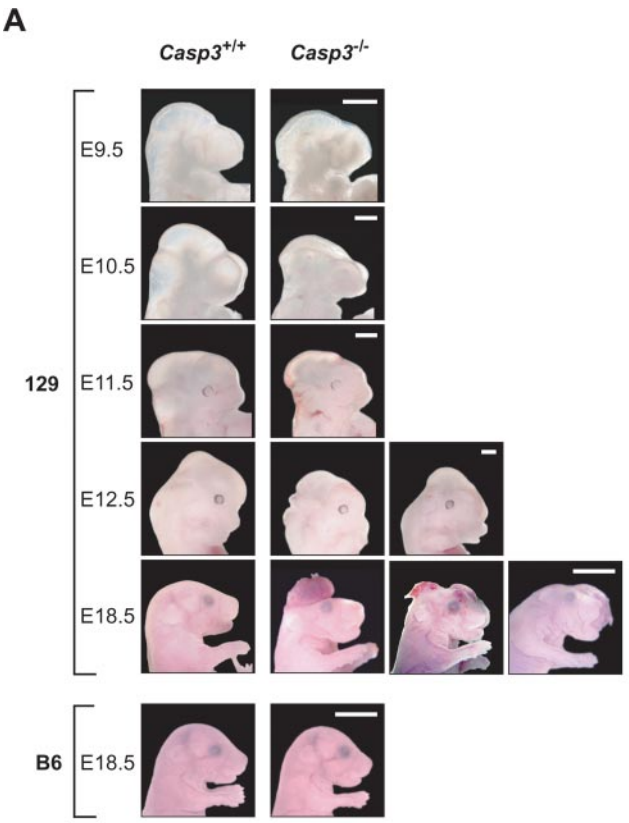

B

Strain	Age	*Casp3*$^{+/+}$ #	*Casp3*$^{+/+}$ (%)	*Casp3*$^{+/-}$ #	*Casp3*$^{+/-}$ (%)	*Casp3*$^{-/-}$ #	*Casp3*$^{-/-}$ (%)	*P* value
129	E18.5	**20**	(21)	**47**	(49)	**29**	(30)	n.s.
	post-natal	**32**	(33)	**62**	(64)	**3**	(3)	<0.0001
B6	E18.5	**18**	(34)	**51**	(60)	**16**	(19)	n.s.
	post-natal	**59**	(30)	**102**	(52)	**36**	(18)	n.s.

Figure 1. 129-*Casp3*$^{-/-}$ but not B6-*Casp3*$^{-/-}$ mouse embryos show brain development defects. *A*, Lateral view of 129- and B6-*Casp3*$^{+/+}$ and *Casp3*$^{-/-}$ mouse embryos. Brain development defects are first evident at E9.5 in 129-*Casp3*$^{-/-}$ embryos. At E18.5, a range of different brain exencephalies are observed. No abnormalities are observed between E18.5 B6-*Casp3*$^{-/-}$ embryos and wild-type littermates. Scale bars: E9.5–E12.5, 100 μm; E18.5, 5 mm. *B*, Genotype frequencies for each strain for E18.5 embryos and postnatal mice. *p* values show that 129-*Casp3*$^{-/-}$, but not B6-*Casp3*$^{-/-}$, are born at a lower than expected Mendelian frequency. n.s., Nonsignificant).

Apoptotic DNA fragmentation is detected in B6-*Casp3*$^{-/-}$ cells and inhibited by a caspase-3-selective inhibitor

Because proper development occurs in B6 mice in the absence of caspase-3, we looked at how DNA fragmentation, a caspase-3 function and apoptotic hallmark, is affected. Primary splenocyte cultures from adult B6-*Casp3*$^{-/-}$ and B6-*Casp3*$^{+/+}$ mice were challenged with 1 mM cycloheximide for 4 hr to induce apoptosis in the presence of increasing concentrations of the caspase-3 inhibitor M-791 (Fig. 2*A*) (Hotchkiss et al., 2000). Apoptotic DNA fragmentation was measured by ELISA. Both B6-*Casp3*$^{+/+}$ and

A

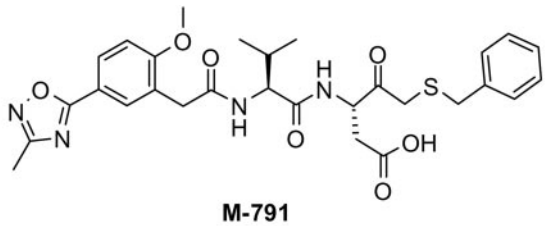

B

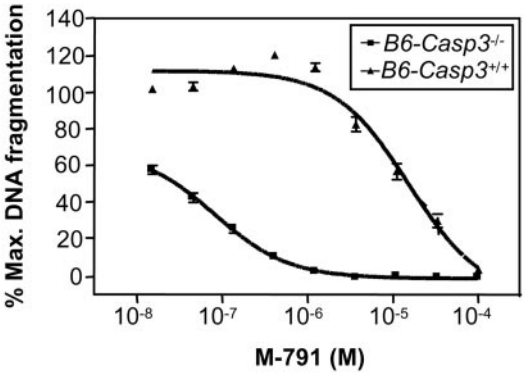

C

		DEVDase activity (AFU/min)	M-791 IC_{50} (nM)
Lung	+/+	316	3.8
	-/-	9.0	8.6
Spleen	+/+	980	7.3
	-/-	6.1	5.3
Liver	+/+	394	6.2
	-/-	8.4	11
Stomach	+/+	557	10
	-/-	9.4	8.5
Brain	+/+	161	3.4
	-/-	1.0	6.9
Kidney	+/+	290	15
	-/-	4.3	14

Figure 2. Caspase-3-like activity is detected in B6-*Casp3*$^{-/-}$ tissues. *A*, Human caspase-3 inhibitor M-791 structure. *B*, Splenocytes isolated from B6-*Casp3*$^{+/+}$ and B6-*Casp3*$^{-/-}$ mice were treated with cycloheximide, with or without indicated concentrations of M-791 simultaneously. DNA fragmentation inhibited by M-791 is detected in both *Casp3*$^{+/+}$ and *Casp3*$^{-/-}$ cells. *C*, B6-*Casp3*$^{+/+}$ and B6-*Casp3*$^{-/-}$ tissue extracts were tested for the presence of DEVDase activity. M-791 potency to inhibit DEVDase activity was measured for each tissue and is shown to be similar in *Casp3*$^{+/+}$ and *Casp3*$^{-/-}$ tissues.

B6-*Casp3*$^{-/-}$ splenocytes underwent DNA fragmentation (Fig. 2*B*). Although the maximum amount of DNA fragmentation in the B6-*Casp3*$^{-/-}$ splenocytes was 60% of that in the B6-*Casp3*$^{+/+}$ splenocytes under the conditions tested, it was fully inhibited by M-791. These results unveil the presence of caspase-3-like activity in *Casp3*$^{-/-}$ splenocytes.

We then verified that this capase-3-like activity, inhibitable by M-791, was present in other tissues by measuring DEVDase activity. Protein extracts were prepared from spleen, lung, liver, stomach, brain, and kidney of adult B6-*Casp3*$^{+/+}$ and B6-*Casp3*$^{-/-}$ mice and tested for their DEVDase activity after pretreatment with the serine protease granzyme B (required to cleave and activate the pool of procaspases in the extracts). DEVDase activity was detected in all B6-*Casp3*$^{-/-}$ tissues tested (Fig. 2*C*) although, as expected, at a lower level than in the B6-*Casp3*$^{+/+}$ tissues. M-791 inhibited the DEVDase activity in both *Casp3*$^{-/-}$ and *Casp3*$^{+/+}$ extracts with comparable IC_{50} values, suggesting that a second enzyme with properties similar to caspase-3 contributed to the M-791-sensitive DEVDase activity.

The caspase-3-like activity in B6-*Casp3*$^{-/-}$ tissues is caspase-7

We used anion-exchange chromatography to isolate this caspase-3-like activity from B6-*Casp3*$^{-/-}$ tissues. Spleen, liver, and kidney cytosolic extracts were preincubated with granzyme B to cleave and activate the pool of inactive procaspases and loaded onto a MonoQ HR 5/5 column. Fractions collected from a NaCl elution gradient were tested for DEVDase activity. A single peak of activity was eluted at 0.2 M NaCl for each of the three tissues assayed (Fig. 3*A* for liver; data not shown for spleen and kidney), which approximates the ionic strength known to be required to elute other caspases from this column type (Nicholson et al., 1995). DEVDase activity-containing fractions obtained from the three organs were pooled and incubated in the presence or absence of biotin-DEVD-AOMK, a biotin-tagged active-site probe for DEVD-recognizing enzymes. Detection by streptavidin-HRP specifically revealed three biotin-labeled polypeptides compared with an unlabeled control (Fig. 3*B*, top, arrowheads). The same three polypeptides were also detected after reblotting the membrane with a monoclonal anti-caspase-7 antibody (Fig. 3*B*, bottom), indicating that the biotin-DEVD-AOMK-labeled proteins were caspase-7.

Note that the migration of the bands in the right lane was slightly retarded because of the additional molecular mass of the biotin-DEVD-AOMK covalently bound to the enzyme. This further confirms that the anti-caspase-7 antibody recognized only proteins that were also biotin-DEVD-AOMK labeled. These results suggest that caspase-7 is the principal enzyme accounting for the DEVDase activity observed in B6-*Casp3*$^{-/-}$ tissues.

M-791 is selective for human caspase-3 but equipotent against mouse caspase-3 and -7

The above-mentioned findings were not consistent with the known potency of M-791 against human caspase-7 (IC_{50} value of 230 nM) (Hotchkiss et al., 2000) versus its potency against the DEVDase activity from B6-*Casp3*$^{-/-}$ tissues (IC_{50}, 5.3–14 nM) (Fig. 2*C*). We thus cloned and purified recombinant mouse caspase-7 and caspase-3 to test whether M-791 would have a different profile against the mouse enzymes. Figure 3*C* shows that M-791 is more potent against mouse caspase-7 than human caspase-7 and equipotent against both mouse and human caspase-3. This further supports the likelihood that caspase-7 is the M-791 inhibitable enzyme with DEVDase and DNA fragmentation activities detected in B6-*Casp3*$^{-/-}$ tissues.

Mouse caspase-7 is as efficient as caspase-3 at cleaving ICAD

Human DNA fragmentation during apoptosis is primarily, if not exclusively, attributable to caspase-3, which cleaves and inactivates ICAD, the inhibitor of the DNase CAD (Wolf et al., 1999). To test whether caspase-7 could mediate this caspase-3 function in mice, we performed *in vitro* cleavage assays with purified mouse and human enzymes on their respective ICAD orthologs. Both mouse and human [^{35}S]-labeled ICAD were transcribed-translated *in vitro* and incubated with the indicated amounts of

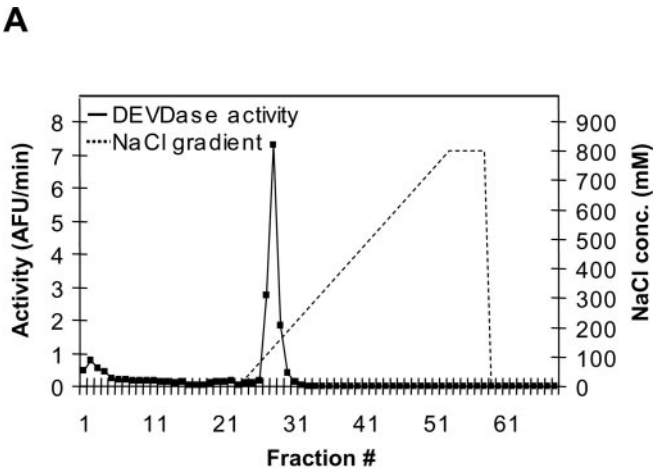

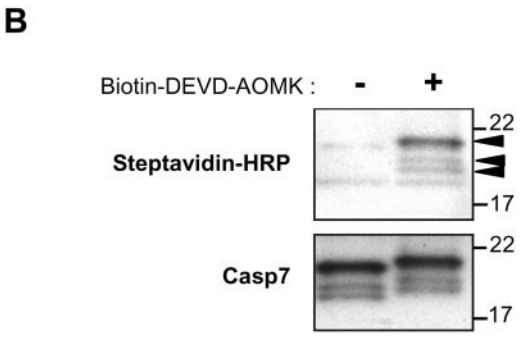

C

Enzymes	Species	M -791 IC_{50} (nM)
Casp7	mouse	31
	human	230
Casp3	mouse	6.5
	human	8.0

Figure 3. The DEVDase activity observed in B6-*Casp3* $^{-/-}$ spleen, liver, and kidney is caspase-7. *A*, DEVDase activity present in B6-*Casp3* $^{-/-}$ tissue lysates was isolated by anion exchange chromatography. A single peak of DEVDase activity was isolated after elution by a NaCl gradient. *B*, Pooled fractions containing DEVDase activity were labeled or not labeled with biotin-DEVD-AOMK. The peptides detected by blotting the labeled sample with streptavidin-HRP (arrowheads, top) are also detected by a monoclonal anti-caspase-7 antibody (bottom). *C*, M-791 potency against purified recombinant human versus mouse caspases-3 and -7 shows species selectivity.

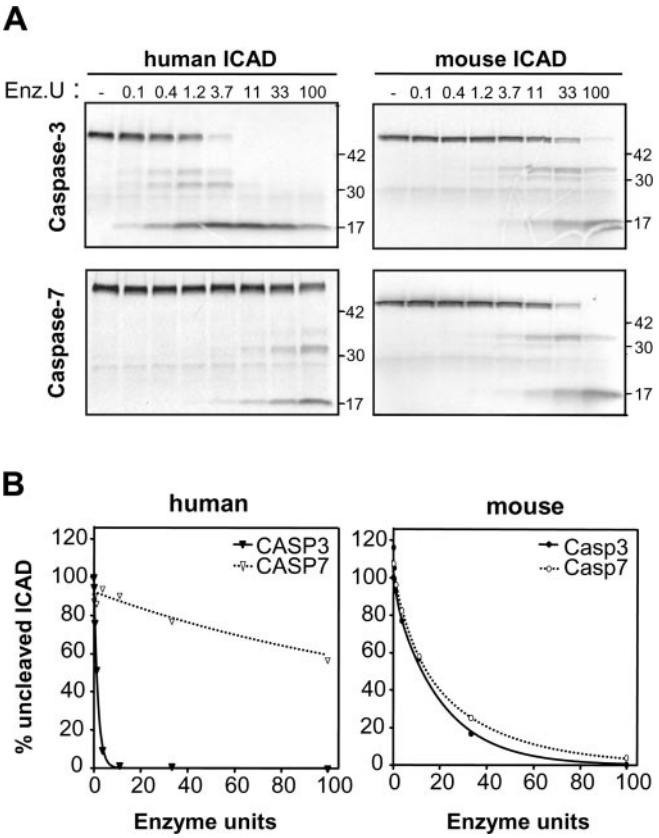

Figure 4. Mouse caspase-7 is more efficient at cleaving ICAD that the human ortholog *in vitro*. *A*, [^{35}S]-labeled *in vitro* transcribed-translated human or mouse ICAD were submitted to cleavage by indicated concentrations of purified human or mouse caspase-3 and caspase-7. *B*, Densitometry of the uncleaved ICAD band in *A* shows that caspase-7 is less efficient than caspase-3 at cleaving ICAD in the case of the human orthologs, but that similar enzymatic cleavage is observed with both mouse caspases. Enz. U, Enzyme units.

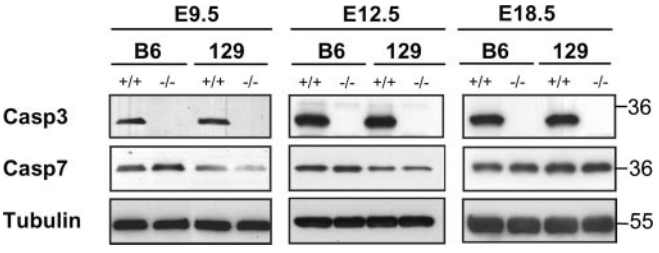

Figure 5. Caspase-7 is differentially expressed in 129 compared with B6 E9.5 embryo heads and E12.5 and E18.5 embryo brains. Western blots of E9.5 embryo head and E12.5 embryo brain lysates show that procaspase-7 is expressed at lower levels in the 129 strain compared with B6, independent of the presence of procaspase-3. This difference is reversed by E18.5. Tubulin is used as an equal loading control.

purified caspase-7 or caspase-3 of the same species. Human caspase-3 was more efficient than human caspase-7 at cleaving human ICAD, as shown by the proteolysis of the p45 full-length ICAD into p34, p28, and p17 (Fig. 4*A*,*B*, left). In contrast, both mouse caspases-3 and -7 were equally efficient at cleaving mouse ICAD (Fig. 4*A*,*B*, right). This supports the possible role of caspase-7 in DNA fragmentation in B6-*Casp3* $^{-/-}$ tissues.

Less caspase-7 is expressed in 129 than in B6 embryonic brain in early development

Data gathered thus far suggest that caspase-7 can mediate at least some caspase-3 functions and, therefore, might be a critical substitute for caspase-3 during B6-*Casp3* $^{-/-}$ brain development. However, caspase-7 fails to do so in the 129 mouse strain. Sequence analysis revealed no differences at critical residues in the caspase-7 and ICAD cDNA sequences between B6 and 129 mice (data not shown). Interestingly, however, B6 embryos expressed 3.5 times more caspase-7 at E9.5 in whole-head tissues and 2.2 times more at E12.5 in the brains than 129 embryos, independently of the presence of caspase-3, as determined by immunoblotting and band density analysis relative to the tubulin loading control (Fig. 5). Caspase-3 protein levels are similar in both wild-type strains. In contrast, at E18.5, caspase-7 is expressed 2.2 times less in brains from B6 embryos compared with brains from 129 embryos. Together, these results support the hypothesis that caspase-7 is a caspase-3 surrogate in *Casp3* $^{-/-}$ mice. Whereas,

in the early stages of brain development, sufficient levels of caspase-7 are present in B6 brains, the decreased amount of caspase-7 in 129 brains is insufficient to compensate for the absence of caspase-3, resulting in a severely abnormal phenotype. Eventually, when the caspase-7 expression increases in the 129 strain, it is probably too late in development for the brain defects too be overcome.

B6-*Casp3*$^{-/-}$ but not 129-*Casp3*$^{-/-}$ precursor neurons can fragment their DNA and activate caspase-7

To assess whether caspase-7 is able to trigger DNA fragmentation during brain development in both strains, despite the differences in basal level expression, we induced apoptosis in precursor neurons isolated from telencephalic vesicles of E12.5 embryos. After overnight culture, cells were challenged with the indicated concentrations of camptothecin for 5 hr to induce apoptosis, and DNA fragmentation was quantified by ELISA. Figure 6*A* shows the fold increase of DNA fragmentation compared with untreated control for the same genotype. Responsiveness to camptothecin-induced apoptotic DNA fragmentation is equivalent in neurons derived from wild-type (*Casp3*$^{+/+}$) and heterozygote (*Casp3*$^{+/-}$) embryos from both B6 and 129 strains ($p > 0.05$). In *Casp3*$^{-/-}$ neurons, however, DNA fragmentation was completely ablated in neurons from 129 embryos but only attenuated in neurons from B6 embryos. Similar results were obtained using staurosporine as the apoptotic agent (data not shown). Western blot analysis of the same cultures monitored for DNA fragmentation showed that less caspase-7 was activated in 129-*Casp3*$^{-/-}$ compared with B6-*Casp3*$^{-/-}$ precursor neurons (Fig. 6*B*). This, in part, is reflective of the intrinsic caspase-7 expression levels in each strain. Together, these data show that apoptotic DNA fragmentation in 129 neurons is dependent on caspase-3, whereas B6 neurons are able to harness their higher levels of endogenous caspase-7 to perform this task.

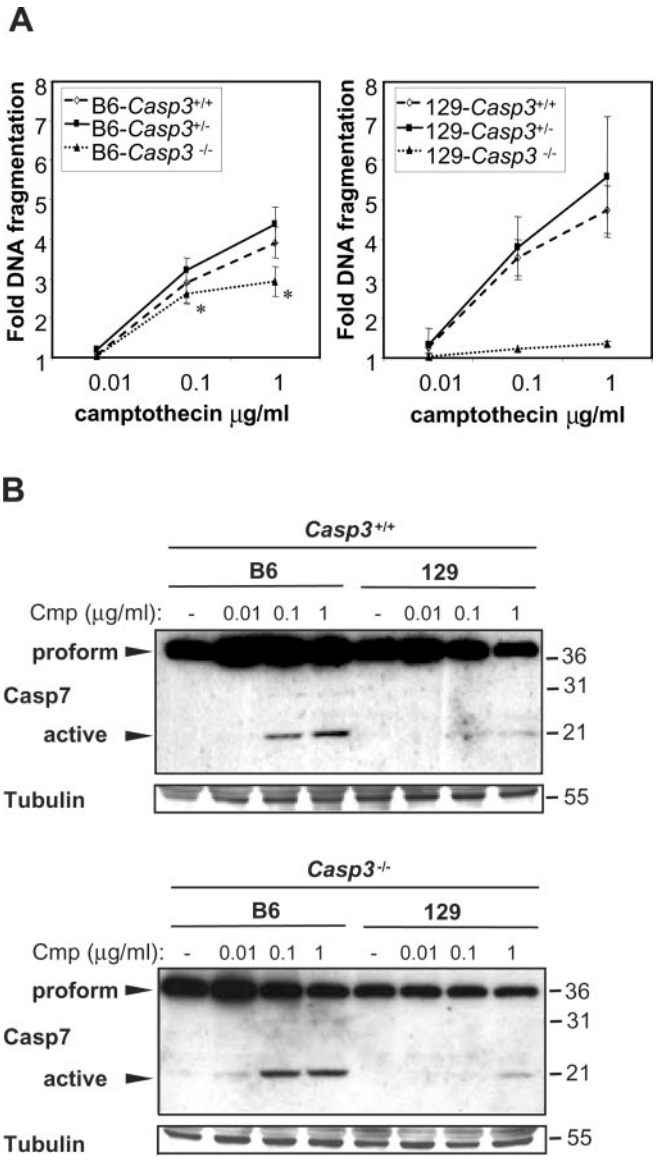

Figure 6. In precursor neurons, DNA fragmentation correlates with higher caspase-7 activation levels in B6-*Casp3*$^{-/-}$ compared with 129-*Casp3*$^{-/-}$. Precursor neurons from E12.5 embryo telencephalic vesicles were maintained in culture for 16–20 hr and then treated with indicated concentrations of camptothecin. *A*, DNA fragmentation was monitored by ELISA. Graphs show the fold increase in DNA fragmentation observed for each camptothecin (Cmp) concentration tested compared with untreated control. Asterisks indicate a significant increase in DNA fragmentation at the 0.1 and 1 μg/ml doses ($p < 0.005$) compared with the 0.01 μg/ml dose for B6-*Casp3*$^{-/-}$ cultures, whereas no significant increase is detected for the 129-*Casp3*$^{-/-}$ cells. For each dose, no significant difference was observed between B6-*Casp3*$^{+/+}$, B6-*Casp3*$^{+/-}$, 129-*Casp3*$^{+/+}$, and 129-*Casp3*$^{+/-}$. *B*, Caspase-7 Western blots show that the activated cleaved form is less abundant in 129 than in B6 cultures for the same camptothecin treatment both in *Casp3*$^{+/+}$ and in *Casp3*$^{-/-}$ cells. Tubulin is used as an equal loading control.

Discussion

Caspases are a family of cysteine proteases involved in apoptosis and inflammation. The caspases involved in apoptosis are divided into the initiator and the executioner caspases depending on how and when they are activated during the cell death program and on their function in cell death events. Some redundancy within these groups has been observed but is not fully understood. For example, executioner caspases-3, -6, and -7 have been shown, in some cases, to cleave the same substrates but with different kinetics or at different sites (Wolf et al., 1999; Slee et al., 2001). Here we report that the requirement for caspase-3 in mouse brain development is dependent on genetic background and expression and activation of caspase-7. We show that mouse caspase-7, in contrast to human caspase-7, exhibits caspase-3-like activity. Mouse caspase-7 cleaves ICAD as efficiently as mouse caspase-3, is differentially activated in proliferating precursor neurons from different strains after camptothecin apoptotic induction, and its activation in *Casp3*$^{-/-}$ neurons correlates with DNA fragmentation. These results suggest that mouse caspase-7 can act as a surrogate in the absence of caspase-3 to allow for normal brain development.

Targeted *caspase-3* deletion in mice of a mixed 129-B6 background results in heterogeneous brain development defects, including brain protrusions through the skull resulting from supernumerary cells (Kuida et al., 1996) and lethality of the embryo or the newborn. In accordance with a previous report (Leonard et al., 2002), we observed that the *Casp3* deletion phenotype is mouse strain specific. B6 mice are resistant to this mutation because they develop and age normally. The 129 strain is more sensitive to *Casp3* deletion than the mixed 129-B6 background, as demonstrated by more severe brain development defects at the gross anatomical level in E18.5 129-*Casp3*$^{-/-}$ embryos. This results in a lower newborn *Casp3*$^{-/-}$ frequency of 3% compared with 7–9% in the mixed background (Kuida et al., 1996; Woo et al., 1998) and 18% in B6.

During brain development, apoptotic cells are detectable in the proliferative neuroepithelium as early as E8.5 (Blaschke et al.,

1996). Because apoptosis occurs in the proliferative zone at early stages, a few progenitor cells escaping death could result in an important accumulation of cells by the end of embryonic development. This is observed in 129-*Casp3*$^{-/-}$ brains, in which gross morphological abnormalities are seen as early as E9.5. However, in other 129 tissues and in the B6 strain, the loss of caspase-3 is compensated for, allowing for well regulated cell death and grossly normal development. Caspase-7, shown in this report to have similar properties to caspase-3 in the mouse, is a good candidate for executing caspase-3-like functions in its absence. Interestingly, the perturbation of apoptosis in the *Casp3*$^{-/-}$ developing brain coincides with low levels of caspase-7 expression in 129 embryo brains compared with the B6 strain. Caspase-7 could thus be expressed at sufficient levels in the B6-*Casp3*$^{-/-}$ embryo to substitute for caspase-3, but its low expression levels would fail to do so in the 129-*Casp3*$^{-/-}$ embryo. This is true at least for the well established caspase-3 function, DNA fragmentation, which cannot be detected when low expression and activation of caspase-7 occurs, as in 129-*Casp3*$^{-/-}$ precursor neurons. In contrast, DNA fragmentation correlates with higher caspase-7 expression and activation in B6-*Casp3*$^{-/-}$ cells.

Depending on the cell model and the apoptotic agent used, it has been controversial in the past whether DNA fragmentation could occur in *Casp3*$^{-/-}$ cells. These studies have been performed in hepatocytes and thymocytes (Zheng et al., 1998), P7 granule neurons (D'Mello et al., 2000), E16.0 and E19.0 neurons (Keramaris et al., 2000) from the mixed 129-B6 background, or the human MCF-7 cell line naturally lacking caspase-3 (Wolf et al., 1999; Mc Gee et al., 2002). Detection of DNA fragmentation in these various models was dependent on the apoptotic agent used, cell type, developmental stage, and sensitivity of the assay used. Unfortunately, none of these previous reports have looked directly at caspase-7 activation nor at its relationship to DNA fragmentation. Caution should also be taken when extrapolating data from human MCF-7 experiments to explain the mouse *Casp3*$^{-/-}$ phenotype, because our data demonstrate that human caspase-7 differs from mouse caspase-7 in its ability to cleave ICAD and relieve the inhibition on DNA fragmentation. The role of caspase-7 in DNA fragmentation has also been demonstrated in chicken cells in which targeted deletion of caspase-7 delays apoptotic DNA fragmentation (Korfali et al., 2004). These findings demonstrate that redundancy in caspase functions is likely to be species dependent. This is of importance when animal models are used to understand human diseases involving the deregulated activation of caspases.

An upregulation in the activation of caspases-6 and -7 has been reported previously in B6-*Casp3*$^{-/-}$ hepatocytes from mice treated with an anti-Fas antibody (Zheng et al., 2000), although proof of functional equivalence with caspase-3 is absent from this study. It is noteworthy that expression and activation levels of caspase-7 are not modified in *Casp3*$^{-/-}$ versus *Casp3*$^{+/+}$ precursor neurons, as described in hepatocytes (Zheng et al., 2000). Others have not observed any apoptosis sensitivity difference between B6-*Casp3*$^{-/-}$ and 129-*Casp3*$^{-/-}$ precursor neurons induced by DNA damage treatments such as cytosine arabinoside and γ-radiation (Leonard et al., 2002), in contrast to the findings reported herein. Thus, differences in sensitivity to apoptosis between B6-*Casp3*$^{-/-}$ and 129-*Casp3*$^{-/-}$ precursor neurons might be stimulus dependent.

In summary, our data demonstrate for the first time the redundancy between caspase-7 and caspase-3 in mediating DNA fragmentation, and thus the potential for caspase-7 to substitute for at least some of caspase-3 functions during mouse brain development. However, we cannot exclude the possibility that other apoptosis-related molecules or some caspase-independent pathways could be differentially regulated in B6 compared with 129 mice, as well. For example, B-cell lymphoma (Bcl)-2, Bcl-X_L, Bax (Bcl-2-associated X protein), Bak (Bcl-Z antagonist/killer), and Bid (BH3-interacting domain death agonist) are pro-apoptotic or anti-apoptotic molecules for which expression also varies throughout development (Krajewska et al., 2002), raising the possibility that a proper balance between the expression of different players in the apoptotic pathways, and not only of one particular caspase, might be critical. A broad genetic study including other backcrossed mouse strains is underway to identify genes other than caspase-7 that may be involved in caspase-3 compensation. As well, a double knock-down of both caspase-3 and caspase-7 on the B6 background would elucidate whether *Casp7* is the only gene mediating the strain-specific *Casp3*$^{-/-}$ phenotype.

References

Blaschke AJ, Staley K, Chun J (1996) Widespread programmed cell death in proliferative and postmitotic regions of the fetal cerebral cortex. Development 122:1165–1174.

Cecconi F, Alvarez-Bolado G, Meyer BI, Roth KA, Gruss P (1998) Apaf1 (CED-4 homolog) regulates programmed cell death in mammalian development. Cell 94:727–737.

D'Mello SR, Kuan CY, Flavell RA, Rakic P (2000) Caspase-3 is required for apoptosis-associated DNA fragmentation but not for cell death in neurons deprived of potassium. J Neurosci Res 59:24–31.

Flaris NA, Shindler KS, Kotzbauer PT, Chand P, Ludwig CP, Konstantinidou AD, Roth KA (1995) Developmentally-regulated lectin binding in the embryonic mouse telencephalon. Brain Res 678:99–109.

Gunn TM, Juriloff DM, Vogl W, Harris MJ, Miller JE (1993) Histological study of the cranial neural folds of mice genetically liable to exencephaly. Teratology 48:459–471.

Hakem R, Hakem A, Duncan GS, Henderson JT, Woo M, Soengas MS, Elia A, de la Pompa JL, Kagi D, Khoo W, Potter J, Yoshida R, Kaufman SA, Lowe SW, Penninger JM, Mak TW (1998) Differential requirement for caspase 9 in apoptotic pathways in vivo. Cell 94:339–352.

Harris MJ, Juriloff DM (1999) Mini-review: toward understanding mechanisms of genetic neural tube defects in mice. Teratology 60:292–305.

Hotchkiss RS, Chang KC, Swanson PE, Tinsley KW, Hui JJ, Klender P, Xanthoudakis S, Roy S, Black C, Grimm E, Aspiotis R, Han Y, Nicholson DW, Karl IE (2000) Caspase inhibitors improve survival in sepsis: a critical role of the lymphocyte. Nat Immunol 1:496–501.

Keramaris E, Stefanis L, MacLaurin J, Harada N, Takaku K, Ishikawa T, Taketo MM, Robertson GS, Nicholson DW, Slack RS, Park DS (2000) Involvement of caspase 3 in apoptotic death of cortical neurons evoked by DNA damage. Mol Cell Neurosci 15:368–379.

Korfali N, Ruchaud S, Loegering D, Bernard D, Dingwall C, Kaufmann SH, Earnshaw WC (2004) Caspase-7 gene disruption reveals an involvement of the enzyme during the early stages of apoptosis. J Biol Chem 279:1030–1039.

Krajewska M, Mai JK, Zapata JM, Ashwell KW, Schendel SL, Reed JC, Krajewski S (2002) Dynamics of expression of apoptosis-regulatory proteins Bid, Bcl-2, Bcl-X, Bax and Bak during development of murine nervous system. Cell Death Differ 9:145–157.

Kuan CY, Roth KA, Flavell RA, Rakic P (2000) Mechanisms of programmed cell death in the developing brain. Trends Neurosci 23:291–297.

Kuida K, Zheng TS, Na S, Kuan C, Yang D, Karasuyama H, Rakic P, Flavell RA (1996) Decreased apoptosis in the brain and premature lethality in CPP32-deficient mice. Nature 384:368–372.

Kuida K, Haydar TF, Kuan CY, Gu Y, Taya C, Karasuyama H, Su MS, Rakic P, Flavell RA (1998) Reduced apoptosis and cytochrome c-mediated caspase activation in mice lacking caspase 9. Cell 94:325–337.

Leonard JR, Klocke BJ, D'Sa C, Flavell RA, Roth KA (2002) Strain-dependent neurodevelopmental abnormalities in caspase-3-deficient mice. J Neuropathol Exp Neurol 61:673–677.

Mc Gee MM, Hyland E, Campiani G, Ramunno A, Nacci V, Zisterer DM (2002) Caspase-3 is not essential for DNA fragmentation in MCF-7 cells

during apoptosis induced by the pyrrolo-1,5-benzoxazepine, PBOX-6. FEBS Lett 515:66–70.

Nagata S, Nagase H, Kawane K, Mukae N, Fukuyama H (2003) Degradation of chromosomal DNA during apoptosis. Cell Death Differ 10:108–116.

Nicholson DW (1999) Caspase structure, proteolytic substrates, and function during apoptotic cell death. Cell Death Differ 6:1028–1042.

Nicholson DW, Ali A, Thornberry NA, Vaillancourt JP, Ding CK, Gallant M, Gareau Y, Griffin PR, Labelle M, Lazebnik YA (1995) Identification and inhibition of the ICE/CED-3 protease necessary for mammalian apoptosis. Nature 376:37–43.

Sakahira H, Enari M, Nagata S (1998) Cleavage of CAD inhibitor in CAD activation and DNA degradation during apoptosis. Nature 391:96–99.

Sakahira H, Iwamatsu A, Nagata S (2000) Specific chaperone-like activity of inhibitor of caspase-activated DNase for caspase-activated DNase. J Biol Chem 275:8091–8096.

Slee EA, Adrain C, Martin SJ (2001) Executioner caspase-3, -6, and -7 perform distinct, non-redundant roles during the demolition phase of apoptosis. J Biol Chem 276:7320–7326.

Thornberry NA, Rano TA, Peterson EP, Rasper DM, Timkey T, Garcia-Calvo M, Houtzager VM, Nordstrom PA, Roy S, Vaillancourt JP, Chapman KT, Nicholson DW (1997) A combinatorial approach defines specificities of members of the caspase family and granzyme B. Functional relationships established for key mediators of apoptosis. J Biol Chem 272:17907–17911.

Vanderluit JL, McPhail LT, Fernandes KJ, McBride CB, Huguenot C, Roy S, Robertson GS, Nicholson DW, Tetzlaff W (2000) Caspase-3 is activated following axotomy of neonatal facial motoneurons and caspase-3 gene deletion delays axotomy-induced cell death in rodents. Eur J Neurosci 12:3469–3480.

Wolf BB, Schuler M, Echeverri F, Green DR (1999) Caspase-3 is the primary activator of apoptotic DNA fragmentation via DNA fragmentation factor-45/inhibitor of caspase-activated DNase inactivation. J Biol Chem 274:30651–30656.

Woo M, Hakem R, Soengas MS, Duncan GS, Shahinian A, Kagi D, Hakem A, McCurrach M, Khoo W, Kaufman SA, Senaldi G, Howard T, Lowe SW, Mak TW (1998) Essential contribution of caspase 3/CPP32 to apoptosis and its associated nuclear changes. Genes Dev 12:806–819.

Wyllie AH (1980) Glucocorticoid-induced thymocyte apoptosis is associated with endogenous endonuclease activation. Nature 284:555–556.

Yoshida H, Kong YY, Yoshida R, Elia AJ, Hakem A, Hakem R, Penninger JM, Mak TW (1998) Apaf1 is required for mitochondrial pathways of apoptosis and brain development. Cell 94:739–750.

Zheng TS, Schlosser SF, Dao T, Hingorani R, Crispe IN, Boyer JL, Flavell RA (1998) Caspase-3 controls both cytoplasmic and nuclear events associated with Fas-mediated apoptosis in vivo. Proc Natl Acad Sci USA 95:13618–13623.

Zheng TS, Hunot S, Kuida K, Momoi T, Srinivasan A, Nicholson DW, Lazebnik Y, Flavell RA (2000) Deficiency in caspase-9 or caspase-3 induces compensatory caspase activation. Nat Med 6:1241–1247.